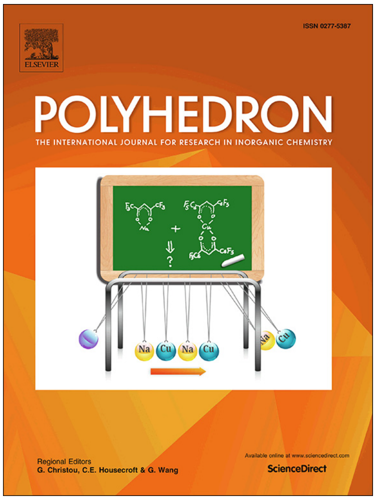

Coordination properties of diethylenetriamine in relation to zinc phthalocyanine

Jan Janczak

PII: S0277-5387(19)30758-2
DOI: https://doi.org/10.1016/j.poly.2019.114313
Reference: POLY 114313

To appear in: *Polyhedron*

Received Date: 5 November 2019
Revised Date: 14 December 2019
Accepted Date: 16 December 2019

Please cite this article as: J. Janczak, Coordination properties of diethylenetriamine in relation to zinc phthalocyanine, *Polyhedron* (2019), doi: https://doi.org/10.1016/j.poly.2019.114313

Coordination properties of diethylenetriamine in relation to zinc phthalocyanine

Jan Janczak

Institute of Low Temperature and Structure Research, Polish Academy of Sciences, Okólna 2 str., P.O.Box 1410, 50-950 Wrocław, Poland

Abstract

The coordination properties of diethylenetriamine (DETA) as a ligand containing three donor nitrogen atoms, two terminal primary amino groups and one secondary central amino group, with respect to divalent zinc ion in ZnPc were examined. The ZnPcDETA complex in the powder form was obtained by the solvothermal reaction of ZnPc with DETA. Recrystallization of the crude product from 3,4-lutidine yields non-centrosymmetric monoclinic solvated crystals $(ZnPcDETA)_3{\cdot}3,4$-lut (**1**) with the space group of Cc. As show the X-ray single crystal analysis in ZnPcDETA complex, the DETA coordinates via terminal amine group to the divalent zinc ion of a planar ZnPc molecule in axial position. Interaction of the N atom of DETA containing a lone electron pair with divalent zinc ion of ZnPc and the formation of the Zn-N coordination bond leads to deviation of the Zn from the N_4-isoindole plane of Pc by ~0.5 Å toward the N-atom of the axial DETA ligand as well as to saucer-shaped distortion of the Pc macrocycle. Arrangement of ZnPcDETA molecules in the 3,4-lutidine solvate crystal with the composition of $(ZnPcDETA)_3{\cdot}$(3,4-lutidine) – (**1**) is determined by the van der Waals forces and by the weak N-H···N hydrogen bonds. The lack of the $\pi\cdots\pi$ interaction between the phthalocyaninate(2-) macrocycles in the crystals (**1**) is clearly evidenced by the Hirshfeld surface analysis, and increases significantly their solubility in most common solvents, even in water, when comparing to the parent ZnPc pigment with limited solubility in solvents and insoluble in water. This feature together with the strong absorption in the therapeutic window within the 600-900 nm makes it a potentially good photosensitizer. DFT calculations performed for the ZnPc-derivatives with DETA, coordinated *via* terminal or central amine group of DETA as well as for the bridged complex (through the terminal amino groups of the DETA ligand of two ZnPc molecules) show the possibility to obtain all three of these complexes. UV-Vis absorption spectra ZnPcDETA complex (**1**) in solutions as well as the diffuse reflectance spectroscopy (DSR) supported by the TD-DFT calculations were used for the characterization of the spectroscopic properties. SHG efficiency of **1** is ~10 % in relation to that of KDP.

Keywords: Zin phthalocyanine; Diethylenetriamine, Crystal structure; Hirshfeld surface DFT; TD-DFT; UV-Vis, SHG

Corresponding author email: j.janczak@intibs.pl

1. Introduction

After the discovery of metallophthalocyanines (MPc's), initially, the interest in them resulted from their deep colour, therefore they began to be used as dyes and pigments [1]. The colour of the metallophthalocyanines results from their chemical structure and their strong absorption in the UV-Vis-NIR range [2]. The MPc's are compounds that contain highly conjugated aromatic macrocycles, consisting of four isoindole units connected together by azamethine nitrogen atoms. Most of metal(II) phthalocyanines have, as a general characteristic, a flat and symmetrical molecular structure, and also exhibit polymorphism [3]. The chemical structure of the metallophthalocyanines as aromatic compounds determine their high thermal and chemical stability, and their flat structure together with the aromatic nature of the Pc-macrocycle determine their poor solubility due to the strong π- π interactions between MPc molecules forming stacking structure in solid [4]. Modification of the substituents attached to the peripheral rings allows for the tuning of the absorption and emission properties of metallophthalocyanines to yield differently coloured dyes and pigments [5]. A large number of phthalocyanines with the majority of metals and some non-metals like as Si or P from the periodic system were obtained and characterized [6]. Besides to their widespread use as dyes and pigments, metallophthalocyanines exhibit many other special properties that are very interesting and therefore there is still interest in this group of compounds. The MPc's have been extensively applied in electronic devices such as gas sensors, nonlinear optics, diodes, transistors, solar cells and photodetectors [7]. For instance, MPc's have been tested in *p-n* junctions for applications in solar cells, leading to excellent conversion efficiency [8]. It must be also mentioned the role played by different metallic atoms at the center of the Pc ring, which leads to a broad range of absorption and emission of these materials within the UV-visible-NIR spectrum [9], besides distinct electrochemical properties when applied as modifier electrodes in electrical catalysis [10], which is of great interest for applications in technological devices. The MPc's have also been applied as dyes for textile shading processes [11], ink jet and laser printing [12] or as materials for CD recordable discs [13]. Furthermore, MPcs have been used as catalysts for the oxidation of methane, phenols, alcohols, polysaccharides, olefins and can also be used to catalyze the transformation of cyano groups in organic cyano compounds [14].

In addition, the metallophthalocyanines, especially the zinc(II) phthalocyanine and its derivatives due to their non-toxicity, are also of prime interest for photodynamic therapy [15]. Their solubility in biological environment is of great importance for application in the biomedical area. This has led to considerable effort to modify the metallophthalocyanines to improve their solubility. The well-known way to tune the application properties of metal(II) phthalocyanine complexes is modify the phthalocyaninato(2-) macroring by the aryl, alkyl, amino, carboxylic, and sulfonic and other substituents [16] or by additive metal center complexation [17]. Both methods improve the solubility of the M(II)Pc-complexes due to the steric hindrance of axial ligands or substituents of hydrogen atoms on phthalocyaninate(2-) macrocycle that lowers the π-π interactions as well as the aggregation in solutions [18]. Several amines, alcohols and other organic compounds containing various donor atoms capable to formation of a donor-acceptor coordinating bond with a metal center of metallophthalocyanines that improve significantly their solubility were investigated [19].

In the present work, diethylenetriamine was selected as the N-donor ligand to investigate its coordination properties towards the central zinc atom in ZnPc. Since the diethylenetriamine contains two different N-donor atoms in the molecule, one central secondary and two terminal primary amine groups, the aim of the work was also to determine the preferences for the coordination of the central divalent zinc in ZnPc by these groups, and to examine its bridging properties with respect to ZnPc with the possibility of the H-type molecules formation as was observed in the case of bipyridine or pyrazine ligands containing two aromatic donor nitrogen atoms in molecule [20].

2. Experimental

2.1. Materials and methods.

Crystalline form of ZnPc was obtained from directly by the reaction of the pure powdered zinc with phthalonitrile as described previously [21]. Diethylenetriamine and 3,4-lutidine were obtained from Aldrich and used without further purification. The composition of the obtained crystals was checked with a Perkin-Elmer 2400 elemental analyser and with energy dispersive spectroscopy (EDS). EDS spectra were acquired and analysed using an EDAX Pegasus XM4 spectrometer with SDD Apollo 4D detector mounted on a FEI Nova NanoSEM 230 microscope. In addition the elemental analysis was carried out also with a Perkin-Elmer 240 elemental analyzer. The Fourier transform infrared spectrum was recorded between 4000 and 450 cm^{-1} on a Bruker IFS 113 V FTIR in a KBr pellets. Thermal analysis was carried out on a Linseis L81 thermobalance apparatus with Pt crucibles. The initial sample mass was about 22 mg. Powder Al_2O_3 was used as a reference. The measurements were performed under static air on heating from room temperature to 300^{o}C at the heating rate of 5^{o}C min^{-1}. The rest of the samples after TG analyses were checked on a PANanalytical X'Pert diffractometer equipped with a Cu-Kα radiation source (λ=1.54182 Å) at room temperature.

2.2. *Synthesis of [ZnPc(dietylenetriamine)]$_3$·3,4-lutidine* (**1**).

Freshly obtained crystalline ZnPc (0.12 g) was added to the diethylenetriamine (15 mL). The suspension of ZnPc in diethylenetriamine was degassed and sealed under reduced pressure in a glass ampoule. Next the ampoule was heated at 160^{o}C for two days and then it was cooled to the room temperature. After such processing the ampoule was opened and filtered. The crude powdered product was added to 25 ml 3,4-lutidine and the suspension was degassed and sealed under reduced pressure in a glass ampoule, and then it was heated for one day at 160^{o}C. Next, the ampoule was cooled to room temperature. After such processes well-developed single crystals of **1** suitable for the single-crystal X-ray analysis were obtained. The crystals of **1** were separated by filtration and dried in air. Yield: 0.106 g (70.5%). Analysis: found: Zn, 8.98; C, 64.41; N, 22.21 and H, 4.40 %. Calculated for $C_{115}H_{96}N_{34}Zn_3$: Zn, 9.12; C, 64.23; N, 22.15 and H, 4.50%. IR (cm^{-1}): 3514^{w}; 3477^{vw}; 3215^{w}; 3197^{w}; 3096^{w}; 3060^{w}; 3028^{vw}; 2961^{w}; 2930^{w}; 1607^{w}; 1579^{w}; 1486^{s}; 1456^{m}; 1339^{m}; 1409^{m}; 1329^{vs}; 1288^{m}; 1084^{vw}; 1162^{m}; 1117^{s}; 1091^{vs}; 1061^{s}; 1023^{m}; 1005^{w}; 949^{w}; 887^{m}; 778^{m}; 750^{s}; 730^{vs}; 633^{w}; 568^{m}; 504^{w}.

2.3. *X-ray crystallography*

The obtained single crystal of **1** was used for data collection on a four-circle KUMA KM4 diffractometer equipped with two-dimensional CCD area detector. The graphite monochromatized Mo-Kα radiation (λ=0.71073 Å) and the ω-scan technique (Δω=1^{o}) were used for data collection. Lattice parameters were refined by the least-squares methods on all reflections positions. One image was monitored as a standard after every 40 images for a control of stability of the crystal. Data collection and reduction along with absorption correction were performed using CrysAlis software package [22]. The structure was solved by direct methods using *SHELXT* [23] giving positions of almost all non-hydrogen atoms. Initially, the structures were refined using *SHELXL-2018/3* [23] with the anisotropic thermal displacement parameters. Hydrogen atoms of the phthalocyanine moiety and 3,4-lutidine were introduced into their geometrical positions and refined as rigid. The H atoms of diethylenetriamine were located on difference Fourier maps, but in the final refinement their positions were constrained (C–H = 0.99 Å for CH_2 groups and N–H = 0.91 Å for coordinated NH_2 and 0.87 Å for central NH and non-coordinated NH_2). Visualizations of the structure was made with the Diamond 3.0 program [24]. Details of the data collection parameters, crystallographic data and final agreement parameters are collected in Table 1.

2.4. *Hirshfeld surface analysis*

Hirshfeld surface analyses, and 2D fingerprint plots as well as percentage contributions for various intermolecular contacts in the investigated crystals were calculated using the Crystal Explorer Ver. 3.1 program package [25].

2.5. *Theoretical calculations*

Molecular orbital calculations with full geometry optimization of zinc phthalocyanine axially coordinated by diethylenetriamine was performed with the Gaussian16 program package [26]. All calculations were carried out using DFT method (Becke3-Lee-Yang-Parr exchange correlation functional B3LYP) [27] with the 6-31G basis set [28] assuming the geometry resulting from the X-ray diffraction study as the starting structure. The calculations were also performed for the substrates ZnPc, diethylenetriamine and 3,4-lutidine molecules. As convergence criterions the threshold limits of 0.00025 and 0.0012 a.u. were applied for the maximum force and the displacement, respectively. The three-dimensional molecular electrostatic potential (3D MESP) maps are obtained on the basis of the DFT (B3LYP/6-31G) optimized geometries of reacted molecules as well as for the reaction product molecules. The calculated 3D MESP is mapped onto the total electron density isosurface (0.008 $eÅ^{-3}$) for each molecule. The colour code of MESP maps is in the range of -0.05 (red) to 0.05 $eÅ^{-1}$ (blue). After the geometry optimization, the time-dependent (TD) DFT calculations [29] were performed to evaluate the absorption spectrum employing the same level and basis sets. All stationary points were optimized without any symmetry assumptions and characterized by normal coordinate analysis at the same level of theory.

2.6. UV-Vis spectroscopy

Measurements of the UV-Vis spectra were carried out at room temperature using an Agilent UV-Vis/NIR Cary 5000 spectrometer. The UV-Vis spectra were recorded diethylenetriamine and 3,4-lutidine solutions ($c = 10^{-6}$ mol/l) whereas in ethanol ($c = 5 \cdot 10^{-7}$ mol/l) and in saturated aqueous solution ($\sim 10^{-8}$ mol/l). Diffuse Reflectance Spectroscopy (DRS) experiments were conducted on Cary-Agilent 5000 spectrometer with the Praying Mantis diffuse reflectance attachment. The powder samples were loaded in a holder with a quartz window and were measured in the region of 200-1100 nm. A powder Al_2O_3 reflectance standard was used as the baseline. To minimize the effects of regular reflection and particle size, the sample was diluted with non- or weak absorbing colorless standard of Al_2O_3. The ratio of the studied ZnPc-derivative complex **1** to the used Al_2O_3 diluent was 1:20, 1:40 and 1:60. The corresponding diluent was also used as the baseline standard. In addition, the same support was also used as diluent as well as standard to examine the effect of the oxide support contribution to the overall DRS spectra. The DRS spectra of the samples were recorded under ambient conditions.

2.6. Second Harmonic Generation measurements

In this study we applied Kurtz-Perry-type technique for semi-quantitative estimation of the SHG efficiency [30]. Prior to measurements compound ZnPcDETA and KDP (potassium dihydrogen phosphate, used as a reference material) were manually crushed and sieved through a mini-sieve set (Aldrich) to a size of 125-177 μm. Prepared in this manner ZnPcDETA and KDP samples were placed between microscope glass slides. Laser pulses were obtained from a laser system consisting of a Quantronix Integra-C regenerative amplifier operating as an 800 nm pump and a Quantronix-Palitra-FS BIBO crystal-based optical parametric amplifier that provides wavelength-tunable pulses of ~130 fs length at the repetition rate of 1 kHz. In this study the output wavelength was set to 1050 nm (mean power of 69 mW), in order to minimize self-absorption effects [31] of pumping and of harmonic radiation (525 nm) by the ZnPcDETA sample. The incident beam was directed onto the plane of sample at about 45 degrees while the detector was placed in front of the sample. Scattered fundamental beam was optically removed with the use of 850 nm shortpass dielectric filter (FESH0850, Thorlabs). The spectra of the emitted second harmonic were recorded by an Ocean Optics 2000 fiber-coupled CCD spectrograph. The geometry of the experimental setup and intensity of the laser beam were the same for ZnPcDETA and KDP. Collection times of 10000 ms and 5000 ms were used for ZnPcDETA and KDP, respectively.

3. Results and Discussion

3.1. Synthesis

Freshly obtained crystalline zinc pthalocyanine by thermal reaction of metal powders with phthalonitrile at 220°C was added diethylenetriamine. The suspension od ZnPc in diethylenetriamine was degassed and sealed under reduced pressure in a glass ampoule. The ampoule was heated at 160°C until a homogeneous solution was obtained (about two days), and next it was slowly cooled to the room temperature at the cooling rate of 5°C h^{-1}. After cooling the powdered product was separated by filtration washed with diethyl ether and dried in air. The elemental analysis of the crude product points on the zinc phthalocyanine with the diethylenetriamine complex with the molar ratio of 1:1. Since the diethylenetriamine contains two different N-donor atoms in the molecule, the question which of amine groups (primary or secondary) forms a coordination bond with central zinc in ZnPc to form a complex with a molar ratio of 1: 1 (Scheme 1), is still opened.

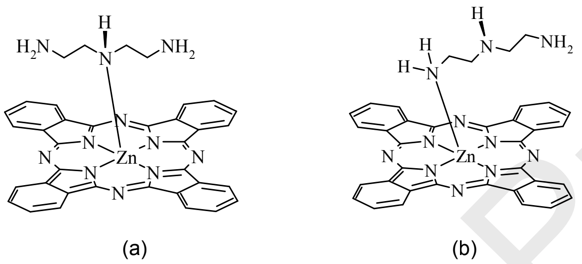

Scheme 1. Two types of ZnPc-complexes formed between the ZnPc and diethylenetriamine with a molar ratio of 1:1.

Therefore, for better understanding the nature of the interaction between the reacted molecules, the three-dimensional molecular electrostatic potential have been calculated [32]. The molecular electrostatic potential (MESP) is related to the electronic density in molecule and is a very useful tool in determining sites for electrophilic and nucleophilic reactions as well as for intermolecular interactions and organisation of molecules in solid-state [33]. The MESP maps of the reacted molecules as well as for the reaction product molecules (Fig. 1) were calculated. The MESP map of ZnPc molecule displays the electrophilic region near the Zn center on both sides of planar ZnPc molecule and the nucleophilic regions near the four bridged azamethine nitrogen atoms. In addition less positive value of MESP than that near the metal center and less negative value of MESP comparing to that of azamethine N atoms are observed on both side of planar molecules across the extended 18π electron conjugation in the Pc(2-) macrocycle (Fig. 1a). The 3D MESP map for diethylenetriamine molecule displays the negative value of MESP near the amine groups pointing the lone electron pair on the N atoms (Fig. 1b). However, the negative region on the MESP for secondary amine group due to the substitution effect of the two ethylene groups is slightly less than that at the primary terminal amino groups. Therefore, the interaction between the ZnPc and diethylenetriamine molecules takes place between the Zn center and one of the amine group. As a result of this interaction, it is possible to form two different types of complexes with a molar ration of 1:1. One of them is a ZnPc complex with a coordinated dietylenetriamine *via* a central secondary amine group, and other type is a complex with the coordinated one of two terminal amino group. Which of the two types of complexes, or perhaps a mixture of both types of complexes, is formed in the above reaction, further structural investigations are needed, the best, on a single crystal using the X-ray diffraction. However, the reaction product of ZnPc with diethylenetriamine has a very fine form of powder, therefore it was recrystallized from various solvents like as pyridine, 3- and 4-methypyridine and 3,4- and 3,5-lutidine, but only from the 3,4-lutidine solution good quality well-developed single crystals suitable for X-ray analysis were obtained. The elemental analysis of the crystals points that the crystals contain, besides the 1:1 complex also solvent molecules. X-ray single crystal analysis revealed that the crystals consist of a ZnPc complex with DETA with a 1:1 molar ratio and additionally contain one solvent molecule (3,4-lutidine) per three molecules of complex. The vibrational spectrum of the obtained crystalline sample performed as KBr pellets exhibits the characteristic bands of Pc macrocycle as well as of the DETA coordinated to Zn center of ZnPc (Fig. S1a in SI). The calculated spectrum for the ZnPcDETA complex (Fig. S1b) is consistent with the experimental spectrum. Moreover, X-ray analysis also showed that during the synthesis, under the conditions used, the ZnPc complex with diethylenetriamine was obtained, in which the coordination bond is formed between the zinc atom ZnPc and one of two terminal amino group of diethylenetriamine. As shown by the MESP maps of ZnPc molecules and diethylenetriamine, it is also possible to form a complex between the ZnPc and a nitrogen atom of the central amino group with a 1: 1 ratio as well as a 2: 1 complex where diethylenetriamine acts as a bridge linking two ZnPc molecules. Therefore, several attempts have been made to obtain ZnPc complex with coordinated diethylenetriamine through the N atom of the central secondary amine group (Scheme 1a) under various temperature and time conditions as well as using different concentration of ZnPc in diethylenetriamine. Additionally, several attempts have also been made to obtain a bridging H-type zinc phthalocyanine complex (scheme 2). The reactions products in all cases were obtained in the powder forms, however, the X-ray diffraction patterns indicated the formation of a mixture of ZnPc-derivatives with DETA. Attempts to their separation and purification still require further investigations.

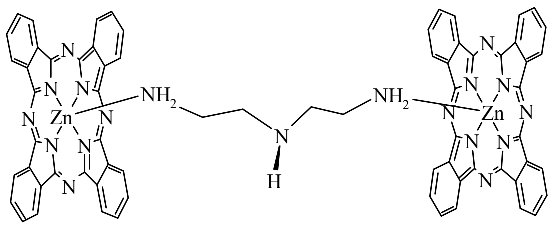

Scheme 2. ZnPc complex bridged by terminal amine groups of diethylenetriamine.

3.2. Thermal properties

In order to determine the thermal stability of obtained compound in crystalline form, the thermal analysis was carried out on the sample of about 25 mg with the heating rate of 5 °C/min. Crystals of the investigated compound, $(ZnPcDETA)_3 \cdot 3,4$-lut, are stable up to ~215°C (See Fig. 2). Above this temperature point, the mass loss of sample indicates the release of the solvated 3,4-lutidine molecule as well as the coordinated diethylenetriamine molecules. Weight loss 19.33% is in agreement with the calculated value of 19.38% associated with a loss of 3,4-lutidine and diethylenetriamine molecules from the sample. Above this temperature the axial Zn–N bond breaks and the diethylenetriamine is release s simultaneously with 3,4-lutidine as a solvent molecule. Finally, the sample gives free ZnPc in the β-form that was confirmed by the X-ray powder diffraction experiment.

3.3. X-ray structural study

The molecular structure of the investigated zinc phthalocyanine derivative was clearly established by the X-ray single crystal analysis. Single crystals suitable for the X-ray diffraction were obtained by recrystallization of a crude product of the reaction of ZnPc and diethylenetriamine from 3,4-lutidine solution. The compound crystallizes in the non-centrosymmetric space group Cc of the monoclinic system. The asymmetric unit of **1** consists of three ZnPcDETA molecules and one 3,4-lutidine solvent molecule (Fig. 3). All independent ZnPcDETA molecules exhibit a similar conformation, in which the divalent zinc ion is coordinated with the four isoindole nitrogen atoms of the phthalocyaninate(2-) macrocycle, and in addition, with the nitrogen atom of one of two terminal amine group of diethylenetriamine as illustrate for the molecule A the Fig. 4. Thus, the coordination polyhedron of the zinc ion exhibits a slightly distorted square pyramid. However, due to the interaction between the zinc of ZnPc and the N atom of amine group of diethylenetriamine and formation of an axial Zn–N bond, the divalent central zinc ion does not lies in the central hole of Pc(2-) as observed in pure ZnPc [34], but is deviated by ~0.54 Å from the plane defined by the four isoindole N atoms of Pc(2-) macrocycle toward to the N atom of axial ligand. The deviation of Zn from the N_4-isoindole plane is very similar in all independent ZnPcDETA molecules (Table 2). As a result of the interaction of the divalent zinc ion of ZnPc with the axial N atom of amine group of diethylenetriamine the planar phthalocyanine macrocycle as found in the β-ZnPc [32] adopts a conformation that is saucer-shaped with a base towards the zinc(II) cation. The deformation of the Pc ring form planarity can be determined by the inclination of the four planar isoindole units to the N_4-plane is ranging from 4.7(2) to 8.8(2), 4.1(2) to 9.6(2) and 4.7(2) to 8.7(2)^o in the independent molecules A, B and C, respectively. The four equatorial Zn–N bonds with Pc(2-) macrocycle are very similar in all independent molecules, but they are longer by ~0.08 Å than those in the β-ZnPc. However, they are still slightly shorter than the axial bond linking the central zinc to diethylenetriamine (Table 2). A search of the Cambridge Structural Database (CSD, Version 5.39) show a similar correlation between the equatorial and axial Zn–N bonds is observed in other 4+1-coordinated ZnPc-derivatives that have been structurally characterized [35].

Arrangement of ZnPcDETA molecules in the crystal depends mainly on the van der Waals forces and the weak hydrogen bonds N-H···N formed between the coordinated amino group (as a donor) and the terminal primary amine group (as an acceptor) of the neighbouring ZnPcDETA molecule (Table 3). The independent molecules A and C are interconnected by weak N–H···N hydrogen bonds with donor-acceptor distances of 3.161(9) and 3.159(8) Å forming chains along the [110] and [-110] directions, whereas the molecules B are interconnected each other *via* N–H···N hydrogen bonds with a donor-acceptor distance of 3.134(9) Å forming chains along the [001] direction (Fig. S2 in the SI). The voids between the chains that are running along [110], [-110] and [001] directions are occupied 3,4-lutidine as solvent molecules. Figure 5 illustrate the packing arrangement of the chains in the unit cell, in which one of the N–H···N hydrogen bonded chain of molecules A and C is marked in red and the N–H···N hydrogen bonded chain of molecules B is marked in blue and the solvent 3,4-lutidine molecules are marked in yellow. The π···π interaction between the phthalocyaninate macrocycles, which is common force determining the arrangement of unsubstituted metallophthalocyanine molecules in the solid-state (crystal) as well as responsible for their limited solubility, in the present structure is absent because the Pc macrocycles are far away from each other.

3.4. Hirshfeld surface analysis

Hirshfeld surface and the analysis of 2D fingerprint plots [36,37] has been used to higher assist the understanding of the numerous intermolecular interactions between the molecules constituting the crystal. The Hirshfeld surface mapped over d_{norm} together with its 2D-fingerprint plot is illustrated in the Figure S3 (in SI) for each independent A, B and C molecules, whereas for whole asymmetric unit of **1** is shown in Figure 6a, in which the blue areas correspond to the contact distance between atoms that are inside (d_i) and outside (d_e) the surface is longer than the sum of the respective van der Waals radii, whereas the red areas correspond to shorter contact distance between atoms that are inside and outside the surface than the sum of the respective van der Waals radii and the white areas of the surface correspond to the contact distance equal to sum of can der Waals radii [38], which identify the regions of the intermolecular interactions. The same interactions display the plot between the d_i *vs* d_e, which referred as 2D-fingerprint plot (Fig. 6b) and the respective fingerprint plot corresponding to the respective interactions (Fig. 6c). The interaction of individual molecules (A, B and C) within the crystal is almost the same as confirmed by the HS and 2D-fingerprint of individual molecules (See Fig. 3a, b and c in SI). The interaction of solvent molecule (3,4-lutidine) present in the crystal has been encompassed in the Crystal Explorer calculations and is illustrated by the HS and its 2D fingerprint plot (see Fig. 3d in SI). The Hirshfeld surface, in particular the 2D fingerprint of the whole asymmetric unit in crystal, is very similar to the 2D-fingerprint of the respective molecules A, B and C (compare the Fig. 6b with the Fig. S2 in SI) what indicates similar types of interactions between individual molecules (A, B and C) as well as between the whole asymmetric units in the crystal. As shown in Figure 6 (as well as Figure S3) the main interactions between whole asymmetric units and between molecules in crystals are the van der Waals interactions, mainly dispersion forces (H···H) with a contribution over 43%, the N···H + H···N with a contribution of 17.0 % resulting from the N–H···N hydrogen bonds and the C···H + H···C interactions with a contribution of 37.8 %. The π···π interaction between the phthalocyaninate(2-) macrocycles are absent between the ZnPcDETA molecules in the investigated crystal. This is in contrast to the β-ZnPc crystal, in which the π···π interaction between planar ZnPc molecules with a contribution of 21.5% is, besides the dispersive forces (H···H), the main force responsible for the stacking arrangement of the ZnPc molecules in crystal (Fig. 7). The absence of the π···π interaction between the ZnPcDETA molecules in the investigated crystals is responsible for the significantly increases their solubility comparing to the parent ZnPc pigment.

3.5. DFT studies

DFT calculations were carried out for the ZnPcDETA molecule in which the diethylenetriamine is coordinated to the zinc center of ZnPc *via* terminal amine group. Fully optimized ZnPcDETA molecule (Fig. 8a) exhibits conformation similar to that in the crystal. In general, the DFT optimised parameters are in good agreement with those observed in the crystals. Selected DFT parameters for the ZnPcDETA molecule is collected together with the X-ray values in the Table 2, whereas the detailed geometrical parameters are listed in Table S1 (in SI). It should be noted that the X-ray experimental results refer to the solid phase and DFT calculated results refer to the conformation of the molecule in the gas phase. Thus, as seen in the Table 2, some differences between these values could be understand. The calculated four equatorial Zn–N bond lengths are in good agreement with the X-ray values, however the axial Zn–N bond is longer by ~0.05 Å that that in the crystal. Similar values of the equatorial N–Zn–N angles are observed for ZnPcDETA molecule in the gas and solid phase, but the X-ray values of the N–Zn–N angles involving the N atom of axial DETA ligand and N-isoindole atoms of Pc(2-) macrocycle have greater differences when compared to that obtained by DFT. The saucer-shape of the Pc ring is less but more regular distorted and the deviation of the divalent zin from the N_4-isoindole plane of Pc macrocycle is smaller by ~0.05 A than those in the crystal due to the intermolecular interaction present in the crystal.

As mentioned in the introduction, the diethylenetriamine molecule contains two different amine groups: primary terminal and secondary central. Both groups with the lone electron pair are able interact with the electropositively polarised divalent zinc ion of ZnPc, as illustrate the 3D MESP maps (Fig. 1), and can form respective ZnPcDETA complexes, in which the central zinc of ZnPc is axially coordinated with primary or secondary amine group of DETA. Additionally, the diethylenetriamine can interacts by its both primary terminal amine groups with two ZnPc molecules resulting the bridged $ZnPcNH_2C_2H_4NHC_2H_4NH_2ZnPc$ complex. Therefore, the DFT calculation of geometries of the complexes have been performed and the results for all ZnPc-derivatives are summarised in the Table 4, and the detailed geometrical parameters for ZnPc-derivatives are listed in Table S2 and S3 (in SI), whereas a view of the molecular structures is illustrated in Fig. 8. As can be seen from the Table 4, for the ZnPc-derivative ligated by a central amine group of DETA the values of equatorial and axial Zn–N bonds are slightly longer than that for the ZnPc-derivative ligated by the terminal group. The equatorial N–Zn–N angles are similar in both ZnPc-derivatives, whereas the angles N-Zn-N involving Si the isoindole N atoms of Pc and the axial N atom of the central amine group of DETA have a greater distribution values than those in the ZnPc-derivative ligated by terminal amine group of DETA. A small differences between the deviation of the divalent Zn ion from the N_4-isondole plane of Pc(2-) macrocycles as well as in the distortion of the Pc(2-) macrocycle form planarity can be found between the ZnPc-derivatives ligated by terminal and central amine group of DETA. For the third molecule, in which DETA acts as a bridge by ligation *via* terminal amino groups of two ZnPc molecules, the DFT calculated coordination environment of divalent Zn ion of both ZnPc molecules is very similar, and the axial Zn–N bonds have an intermediate values (2.1680 and 2.1699 Å) between the Zn-N values of ZnPc-derivatives ligated by terminal (2.1403 Å) or central (2,1901 Å) amine group of DETA (Table 4). These small differences in the lengths of bonds between divalent zinc ion of ZnPc and the amine groups from DETA are also reflected in the differences between the energies of these bonds. The calculated energies of the axial Zn–N bonds are 134.1 kJ/mol for the ZnPc-derivative ligated by N atom of terminal amine of DETA and 129.1 kJ/mol for the ZnPc-derivative ligated by N atom of central amine of DETA, whereas the value of the sum energies of two Zn–N bonds of for the ZnPc-derivative bridged two ZnPc molecules by terminal amine groups of DETA is equal 239.2 kJ/mol (Zn1–N9 = 120.1 kJ/mol and Zn1–N11 = 119.1 kJ/mol, for numbering of atoms see Fig.8c). The calculated energy of the axial Zn–N bond in these ZnPc-derivatives with DETA is smaller than the calculated binding energy of 5.66 eV (~546.3 kJ/mol) between the divalent zinc center and the phthalocyaninate macrocycle [39]. The calculated energy of the molecule of ZnPc-derivative ligated by N atom of terminal amine of DETA is lower by ~28.1 kJ/mol than that of the molecule of ZnPc-derivative ligated by N atom of central amine of DETA. Furthermore, as shown by the DFT calculations, all three ZnPc-derived molecules ligated or bridged by DETA are possible to obtain.

3.6. UV-Vis spectroscopic characterization

To further characterize of ZnPc-derivative ligated by N atom of terminal amine of DETA , the electronic absorption spectra were recorded. Since the crystalline sample of **1** as shows single crystal analysis contains ZnPcDETA and 3,4-lutidine molecules, therefore the UV-Vis spectra were recorded in diethtlenetriamine and in 3,4-lutidine solutions (Fig. 9a). In addition, due to the relatively good solubility of the investigated ZnPc-derivative (**1**) in ethanol as well as in water, despite its limited solubility, the UV-Vis spectra in these solvents were measured (Fig. 9b). The spectrum of the investigated ZnPc-derivative (**1**) in all solvents shows two bands (Q and B) characteristic for the phthalocyaninate(2-) macrocycle [40]. The Q and B bands are observed at ~670 and ~350 nm in all used solvents (Fig. 9). The Q band corresponds to the excitation between the HOMO to LUMO level and the B band corresponds to the HOMO-1 to LUMO level. In addition, the vibrionic splitting of the Q band with a splitting value of ~60 nm is observed, what was mentioned in the literature [41]. Besides, the UV-Vis spectroscopic characterization of the investigated ZnPc-derivative (**1**) in solutions, the diffuse reflectance spectroscopic (DSR) characterization on solid of ZnPc-derivative (**1**) was performed. Due to the high diffuse reflectance of the ZnPc-derivative (**1**) and to minimize the effects of regular reflection and particle size, the sample was diluted with non- or weak absorbing colorless standard of Al_2O_3. The ratio of the studied ZnPc-derivative complex (**1**) to the used Al_2O_3 diluent was 1:20, 1:40 and 1:60. As shown in Figure 10, DSR spectra of complex **1** independent of the concentration of the studied complex in Al_2O_3 exhibit quite similar bands with intensities depending on the concentrations of the complex **1** in Al_2O_3. The λ_{max} of the Q and B bands are observed at 671 and 348 nm, which are quite similar to that observed for the complex **1** in solutions. However, due to the interactions between molecules of ZnPc-derivative in solid, DSR bands are significantly much wider in relation to that for the UV-Vis bands of the complex **1** in solutions. The broadening of absorption bands in solid thin films a common feature of metallophthalocyanines, which was widely discussed in the literature [42].

To investigate further the optical properties of the ZnPcDETA complex **1** the time-dependent TD DFT calculations have been performed. Optical absorption spectrum was calculated for the ZnPcDETA with ligated by terminal amine group of DETA as well as for the parent ZnPc pigment, for a comparison. The results are summarized in Table 5 and the full details are listed in Tables S4 and S5 (SI). Partial molecular energy diagram, HOMO and LUMO frontiers orbitals and the calculated electronic absorption spectra for ZnPcDETA and ZnPc are shown in Figure 11. The calculated energy gap between HOMO and LUMO levels is 2.0251 eV (612 nm) for the ZnPcDETA complex, whereas for the parent ZnPc complex is 2.0857 eV (594 nm). A small bathochromic shift of the maximum absorption wavelength (λ_{max}) of the dye molecule was observed, as the DETA was bonded to the divalent zinc centre of ZnPc. The blue-shift of 18 nm is related with the slightly decreasing of the energy gap in relation to ZnPc that should be assigned to the ligation effect of the DETA molecule as well as to the saucer-shaped distortion of phthalocyaninate macrocycle. The TD DFT calculated HOMO-LUMO transition for the ZnPcDETA as well as for ZnPc complexes is shifted by ~60 nm in relation to that of the experimental values. Quite similar discrepancy between the experimental and theoretical results are found also for the other metallophthalocyanines [43]. There are large number of work reporting the DFT and TD DFT calculations performed on tetrapyrrole systems like as porphyrin, porphyrazin, phthalocyanine, naphthalocyanine and their metal complexes [44], the TD DFT reporting the unsubstituted zin phthalocyanine and its axially ligated derivative are relatively rare [45]. Aromatic macrocycles including metallophthtalocyanines, especially zin phthalocyanine and their derivatives due to their non-toxicity are extensively studied as photosensitizers in photodynamic therapy [46]. The photosensitizer should have a strong absorption in the therapeutic window of 600-900 nm. The ZnPcDETA complex investigated here, as shown the UV-Vis spectrum, due to its slightly solubility in water, can be used as photosensitizer for PDT, since it can be introduce do the tissue. In PDT, a photosensitizer in its ground state (S_0) firstly absorbs energy and is excited to its short-lived first excited state (S_1), than undergoes conversion to the first excited triplet state by intersystem crossing. The triplet state of photosensitizer can release its energy to the surrounding biological tissue exciting the oxygen from its triplet ground state to the highly active singlet state, that will kill targeted cells. The investigated here ZnPcDETA complex have a strong absorption band in the therapeutic window and the HOMO-LUMO energy gap is sufficient to excite the ground state of oxygen and therefore it can be tested as potential photosensitizer in PDT.

TD DFT calculations were also performed for ZnPc-derivatives ligated by the central secondary amino group of the DETA ligand as well as the bridge-complex, ZnPcDETAZnPc, and the results are listed in Table S6 and S7 (in SI), respectively. Partial molecular energy diagram, HOMO and LUMO frontiers orbitals and the calculated electronic absorption spectra for these two complexes are shown in Fig. S4 (SI). For the ZnPcDETA complex ligated by the central secondary amine group of DETA, the calculated energy gap between HOMO and LUMO levels is 2.1099 eV (588 nm) and is slightly shifted in relation to the HOMO-LUMO gap of the parent ZnPc complex (2.0857 eV, 594 nm), whereas for the bridge-complex, ZnPcDETAZnPc, the calculated gap between the HOMO and LUMO levels (2.0817 eV , 596 nm) is almost compared with the gap between the HOMO-1 and LUMO+1 levels (2.0976 eV, 591 nm). Additionally, in the TD-DFT UV-Vis spectrum of ZnPcDETA complex ligated by the central secondary amine group of DETA, the band associated with HOMO-2 and LUMO+1 transition (3.2479 eV, 382 nm) is observed with intensity two times greater than that in the ZnPcDETA complex ligated by terminal amine. Concluding, the TD DFT calculations performed for these ZnPc-derivatives show bathochromic shift of the Q band in the ZnPc-derivative ligated by terminal amine group of DETA ligand (612 nm) and hypsochromic shift in the ZnPc-derivative ligated by central secondary amine group of DETA ligand (588 nm), whereas for the bridge-complex the position of Q band due to the overlap of two transitions (596 and 591 nm) is almost unchanged in relation to that in the calculated spectrum of the parent ZnPc (594 nm).

3.7. Nonlinear optical properties.

As is known, only the non-centrosymmetric structures might have a second-order nonlinear optical effect [47]. Metallophthalocyanines (MPc's), with their highly polarizable two-dimensional 18π-electron system, are known for their good second-order NLO properties especially when unsymmetrically substituted [48]. Although the investigated ZnPcDETA complex contains the unsubstituted phthalocyaninate(2-) macrocycle, but it crystallizes in a non-centrosymmetric space group (*Cc*), therefore the SHG was measured using the laser pulses at 1050 nm. The spectra of the emitted second harmonic were recorded by an Ocean Optics 2000 fiber-coupled CCD spectrograph. The result obtained from a powdered sample of the $(ZnPcDETA)_3{\cdot}3,4$-lut crystals (**1**) in the form of a pellet (Kurtz powder test) were compared with those obtained for KDP (see Fig. S5 in SI) and confirms its non-centrosymmetric space group. The experimental results revealed that the sample of **1** display powder SHG efficiency of approximately 10% of that of potassium dihydrogen phosphate (KDP).

4. Conclusion

The coordination properties of dietylenetriamine toward to zinc of ZnPc were investigated. The ZnPc-derivative with dietylenetriamine coordinated to the divalent zinc ion *via* terminal primary amine group was obtain in the crystalline form as 3,4-lutidine solvate $[ZnPc(DETA)]_3{\cdot}3,4$-lutidine. Single crystal analysis of the $[ZnPc(DETA)]_3{\cdot}3,4$-lutidine compound shows that the there are no $\pi{\cdots}\pi$ interactions between the phthatlcyaninate(2-) macrocycles of ZnPc(DETA) molecules. The $\pi{\cdots}\pi$ interaction is common feature of metallophthalocyanines in solids. This feature was clearly evidenced by the HS analysis. The lack of $\pi{\cdots}\pi$ interaction between ZnPc(DETA) molecules in the solid state results in a significant increasing of its solubility, even in water, compared to the parent ZnPc pigment, which is insoluble in water. This feature together with a strong absorption in the therapeutic window of 600-900 nm make it a good photosensitizer. DFT calculations performed for the ZnPc-derivatives with DETA, coordinated via terminal or central amine as well as for the bridged by terminal amine groups of DETA two ZnPc molecules show the possibility to obtain all three of these complexes. The ZnPcDETA complex with a coordinated terminal amino group of DETA is energetically more favorable (by ~28.1 kJ/mol) than in the complex with coordinated by the central secondary amine group. ZnPcDETA complex in the solid phase as shown by DSR as well as in solutions as shown by UV-Vis absorption spectra exhibits good color properties and can be used as a dye or pigment. The ZnPcDETA complex that crystallizes in the non-centrosymmetric space group of the monoclinic system (*Cc*) as 3,4-lutidine solvate $(ZnPcDETA)_3{\cdot}3,4$-lut exhibits NLO properties with the SHG efficiency of approximately 10% of that of potassium dihydrogen phosphate (KDP).

5. Supplementary material

Additional material contains the experimental calculated IR spectra, additional figures illustrated the chains of ZnPcDETA molecules and HS for all independent ZnPcDETA molecules (A, B and C) and for the parent ZnPc, the comparison of the efficiency of the SHG for ZnPcDETA with KDP, the partial molecular energy diagram, HOMO and LUMO frontiers orbitals and the calculated absorption spectra for the ZnPc(DETA) ligated *via* central amine group of DETA and bridged by terminal amine groups of DETA complex, ZnPc(DETA)ZnPc, as well as the DFT optimized parameters and the TD DFT output files for the ZnPcDETA derivatives. Full details of the X-ray data collection and final refinement parameters including anisotropic thermal parameters and full list of the bond lengths and angles for $(ZnPcDETA)_3\cdot 3,4$-lut (**1**). have been deposited with the Cambridge Crystallographic Data Center in the CIF format as supplementary publications no. CCDC 1962350. Copies of the data can be obtained free of charge on the application to CCDC, 12 Union Road, Cambridge, CB21EZ, UK, (fax: (+44) 1223-336-033; email: deposit@ccdc.cam.ac.uk).

Acknowledgment

DFT and TD DFT calculations have been carried out using resources provided by Wrocław Centre for Networking and Supercomputing (http://www.wcss.wroc.pl).

Table 1. Crystallographic data for (ZnPcDETA)$_3$·3,4-lut (**1**).

	1
Formula	$C_{115}H_{96}N_{34}Zn_3$
Molecular weight	2150.43
Crystal system	monoclinic
Space group	*Cc*
a (Å)	24.9997(9)
b (Å)	23.5003(8)
c (Å)	16.8698(7)
β (°)	95.285(5)
V (Å^3)	9868.9(6)
Z	4
$F(000)$	4456
$D_{\mathrm{calc}}/D_{exp}$ [gcm^{-1}]	1.379 / 1.375
μ (mm^{-1})	0.108
Crystal size (mm^3)	0.38 × 0.30 × 0.24
Absorption correction	multi-scan
$T_{\mathrm{min}}/T_{\mathrm{max}}$	0.7892 / 1.000
Total / Unique / Obs refls	100128 / 24483 / 19338
R_{int}	0.0624
R, wR [$F^2>2\sigma(F^2)$]^a	0.0612
R, wR [F^2 all refls]^b	0.1537
S	1.033
Flack parameter	0.017(9)
$\Delta\rho_{\mathrm{max}}$, $\Delta\rho_{\mathrm{min}}$ (e·Å^{-3})	1.396, -0.960

[a] $R=\Sigma\,||F_o|-|F_c||/\Sigma F_o$; [b] $wR=\{\Sigma\,[w(F_o^2-F_c^2)^2]/\Sigma wF_o^4\}^{½}$; $w^{-1}=\sigma^2(F_o^2)+(aP)^2+bP$ where $P=(F_o^2+2F_c^2)/3$. The a and b parameter are 0.0717 and 12.0351.

Table 2. Selected geometrical parameter (Å,°) for (ZnPcDETA)$_3$·3,4-lut (**1**).

	X-ray			DFT
	Mol. A	Mol. B	Mol. C	
Zn1—N2	2.066(5)	2.067(5)	2.069(5)	2.0595
Zn1—N4	2.058(5)	2.055(5)	2.055(5)	2.0636
Zn1—N6	2.044(5)	2.052(5)	2.045(5)	2.0572
Zn1—N8	2.051(5)	2.056(5)	2.057(5)	2.0567
Zn1—N9	2.092(5)	2.097(5)	2.098(5)	2.1403
N2—Zn1—N4	85.9(2)	86.2(2)	86.1(2)	87.01
N4—Zn1—N6	86.19(19)	85.7(2)	85.7(2)	86.53
N6—Zn1—N8	86.84(19)	87.1(2)	87.3(2)	87.15
N8—Zn1—N2	85.77(19)	85.1(2)	85.1(2)	86.94
N2—Zn1—N9	98.1(2)	98.1(2)	99.1(2)	101.88
N4—Zn1—N9	104.9(2)	105.9(2)	105.7(2)	99.90
N6—Zn1—N9	111.6(2)	112.2(2)	111.0(2)	104.30
N8—Zn1—N9	105.0(2)	104.7(2)	104.8(2)	106.63
Deviation of Zn from N_4-plane	0.531	0.542	0.540	0.469
ϕ_1 *)	5.1(2)	4.5(2)	7.3(2)	5.10
ϕ_2	8.4(2)	9.5(2)	8.7(2)	5.09
ϕ_3	4.7(2)	4.1(2)	4.7(2)	6.12
ϕ_4	8.8(2)	9.6(2)	8.0(2)	6.19

*) ϕ_1, ϕ_2, ϕ_3 and ϕ_4 angles are is defined as the angle between the isoindole rings, (N2,C1÷C8), (N4,C9÷C16), (N6,C17÷C24) and (N8,C25÷C32), and the N_4-plane of the Pc that characterize the saucer-shape of Pc macrocycle.

Table 3. Hydrogen-bond geometry (Å, °).

D—H···*A*	*D*—H	H···*A*	*D*···*A*	*D*—H···*A*
N9A—H92···N11C	0.91	2.31	3.161(9)	155
N9B—H93···N11B^{i}	0.91	2.27	3.134(9)	158
N9B—H94···N10B	0.91	2.53	2.970(9)	110
N9C—H95···N11A^{ii}	0.91	2.31	3.159(8)	155

Symmetry codes: (*i*) *x*, −*y*+1, *z*−1/2; (*ii*) *x*+1/2, *y*+1/2, *z*.

Table 4. Comparison of DFT selected geometrical parameter (Å,°) for ZnPc complexes with dietylenetriamine.

	ZnPc coordinated by terminal amine of DETA	ZnPc coordinated by central amine of DETA	bridged by terminal amine groups of DETA of two ZnPc
Zn1—N2	2.0595	2.0809	2.0678 / 2.0575[c]
Zn1—N4	2.0636	2.0723	2.0611 / 2.0605
Zn1—N6	2.0572	2.0474	2.0444 / 2.0528
Zn1—N8	2.0567	2.0542	2.0529 / 2.0517
Zn1—N9	2.1403	2.1901 (N10)[a]	2.1680 / 2.1699 (N11)
N2—Zn1—N4	87.01	86.07	86.69 / 86.95
N4—Zn1—N6	86.53	86.75	87.34 / 87.28
N6—Zn1—N8	87.15	87.38	87.59 / 87.16
N8—Zn1—N2	86.94	86.50	86.95 / 87.34
N2—Zn1—N9[a]	101.88	94.81 (N10)[a]	96.67 / 102.24 (N11)
N4—Zn1—N9	99.90	96.74 (N10)	99.26 / 99.84 (N11)
N6—Zn1—N9	104.30	113.76 (N10)	109.09 / 103.33 (N11)
N8—Zn1—N9	106.63	109.69 (N10)	106.48 / 105.71 (N11)
Deviation of Zn from N_4-plane	0.469	0.479	0.461 / 0.455
ϕ_1[b]	5.10	5.50	0.30 / 5.70
ϕ_2	5.09	5.79	6.09 / 4.11
ϕ_3	6.12	5.09	6.39 / 5.49
ϕ_4	6.19	7.00	6.30 / 5.89

[a] for ZnPc coordinated by central amine of DETA the axial N is N10 (see Fig. 8b);

[b] ϕ_1, ϕ_2, ϕ_3 and ϕ_4 angles are is defined as the angle between the isoindole rings, (N2,C1÷C8), (N4,C9÷C16), (N6,C17÷C24) and (N8,C25÷C32), and the N_4-plane of the Pc that characterize the saucer-shape of Pc macrocycle;

[c] for bridged the values are for respective Zn1 and Zn1′ atoms (se Fig. 8c).

Table 5. TD-DFT results for the low-energy π-π states for ZnPc(DETA) and ZnPc for a comparison.

(a) ZnPc(DETA)

λ, nm	E, eV	*f*	Contribution (weight, %)*)
606.58	2.0440	0.4054	176→177 (94.0), 174→178 (6.4)
602.01	2.0595	0.3977	174→177 (93.7), 176→178 (6.5)
373.08	3.3232	0.0491	173→178 (49.7), 174→178 (17.2), 173→177 (9.7), 172→177 (5.3)
372.99	3.3241	0.0502	173→177 (46.3), 171→177 (10.8), 174→177 (10.4), 173→178 (9.4)
369.89	3.3519	0.0096	172→178 (84.4), 171→178 (5.2), 174→178 (2.2)
368.66	3.3631	0.0043	175→177 (84.4), 171→177 (10.4)
365.91	3.3884	0.0260	171→177 (58.0), 175→177 (13.4), 169→177 (9.2), 174→177 (4.9), 173→177 (4.3)
363.55	3.4104	0.0004	176→179 (86.0), 172→177 (3.9)

*) HOMO (176), LUMO (177)

(b) ZnPc

λ, nm	E, eV	*f*	Contribution (weight, %)*)
594.46	2.0857	0.4084	147→148 (93.8), 145→149 (6.6)
594.43	2.0858	0.4085	147→149 (93.8), 145→148 (6.6)
373.77	3.3171	0.0137	146→148 (90.6), 137→148 (6.7)
373.77	3.3171	0.0137	146→149 (90.5), 137→149 (6.7)

*) HOMO (147) and LUMO (148)

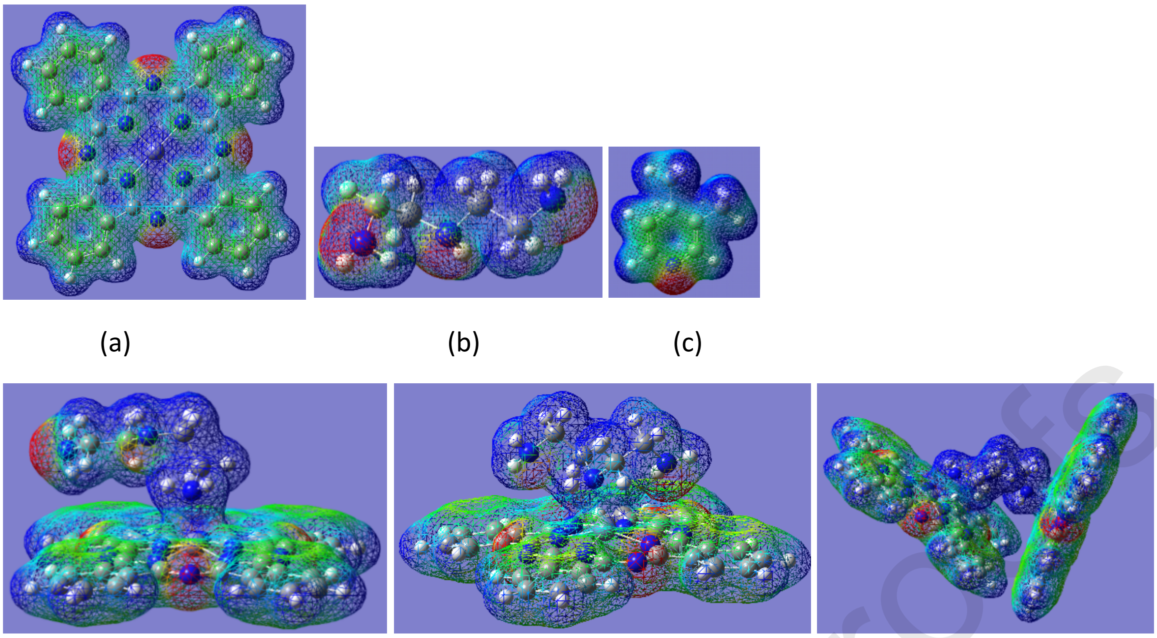

(a) (b) (c)

(d) (e) (f)

Figure 1. The calculated 3D MESP is mapped onto the total electron density isosurface (0.008 e$Å^{-3}$) for ZnPc (a), diethylenetriamine (b), 3,4-lutidine (c) and ZnPc(DETA) coordinated by terminal (d) and central amine (e) and the bridged (f). The colour code of MESP is in the range of –0.05 (red) to 0.05 e$Å^{-1}$ (blue).

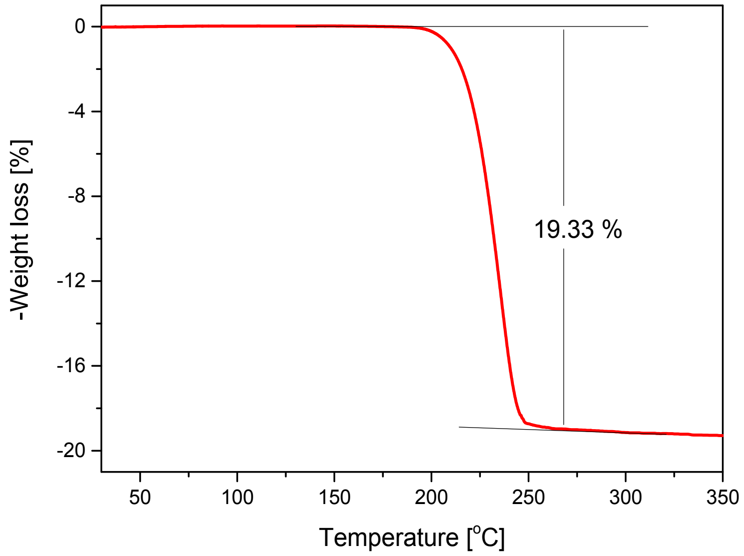

Figure 2. Thermogram for the $[ZnPc(DETA)]_3 \cdot 3,4$-lut.

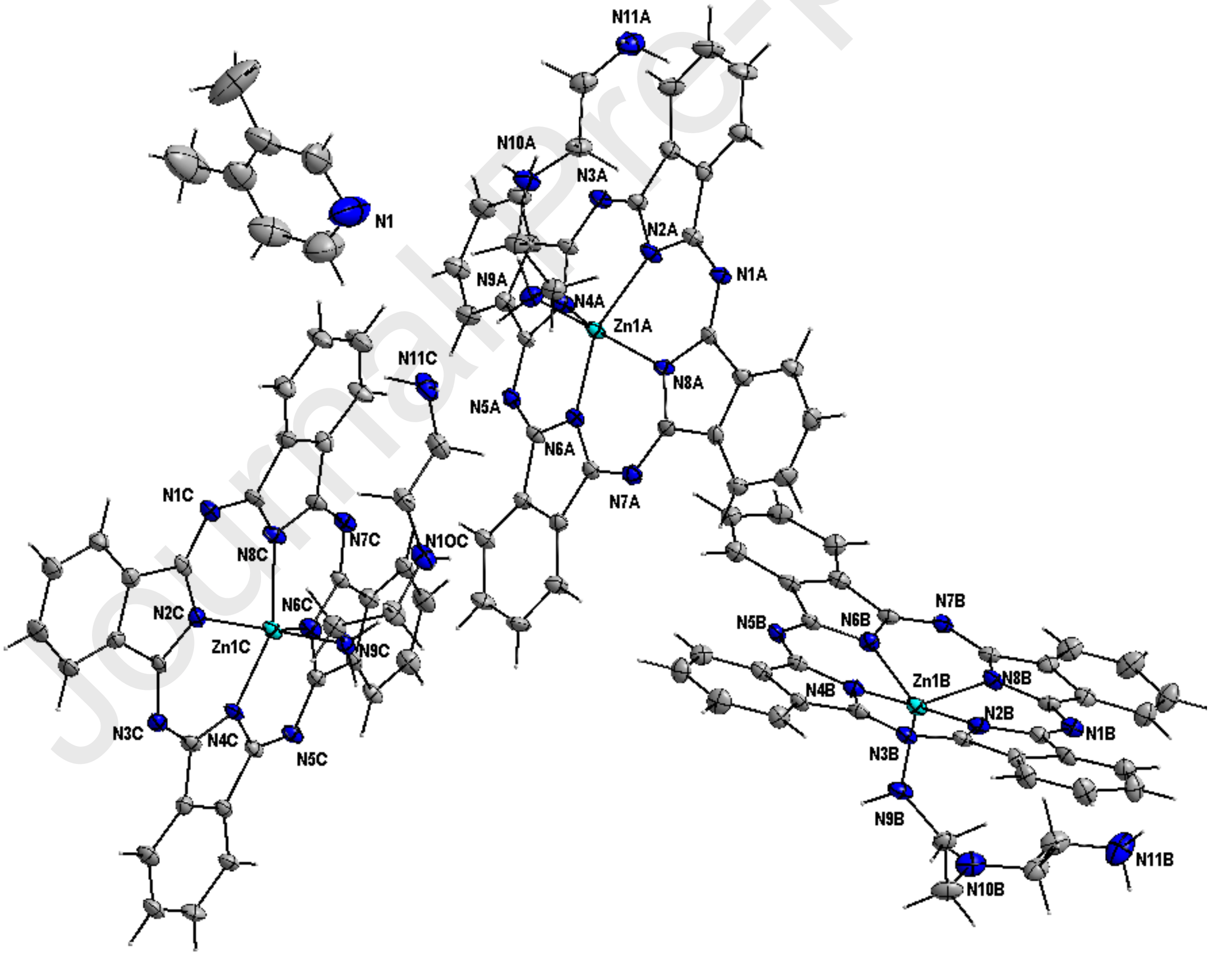

Figure 3. View of the asymmetric unit of **1**.

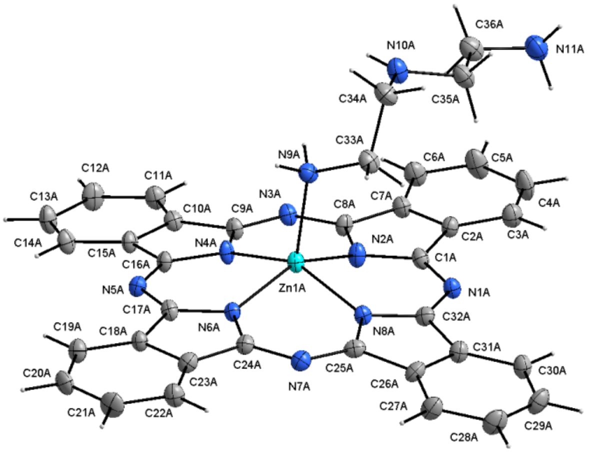

Figure 4. View of one of the three asymmetric unit of ZnPcDETA (Mol. A).

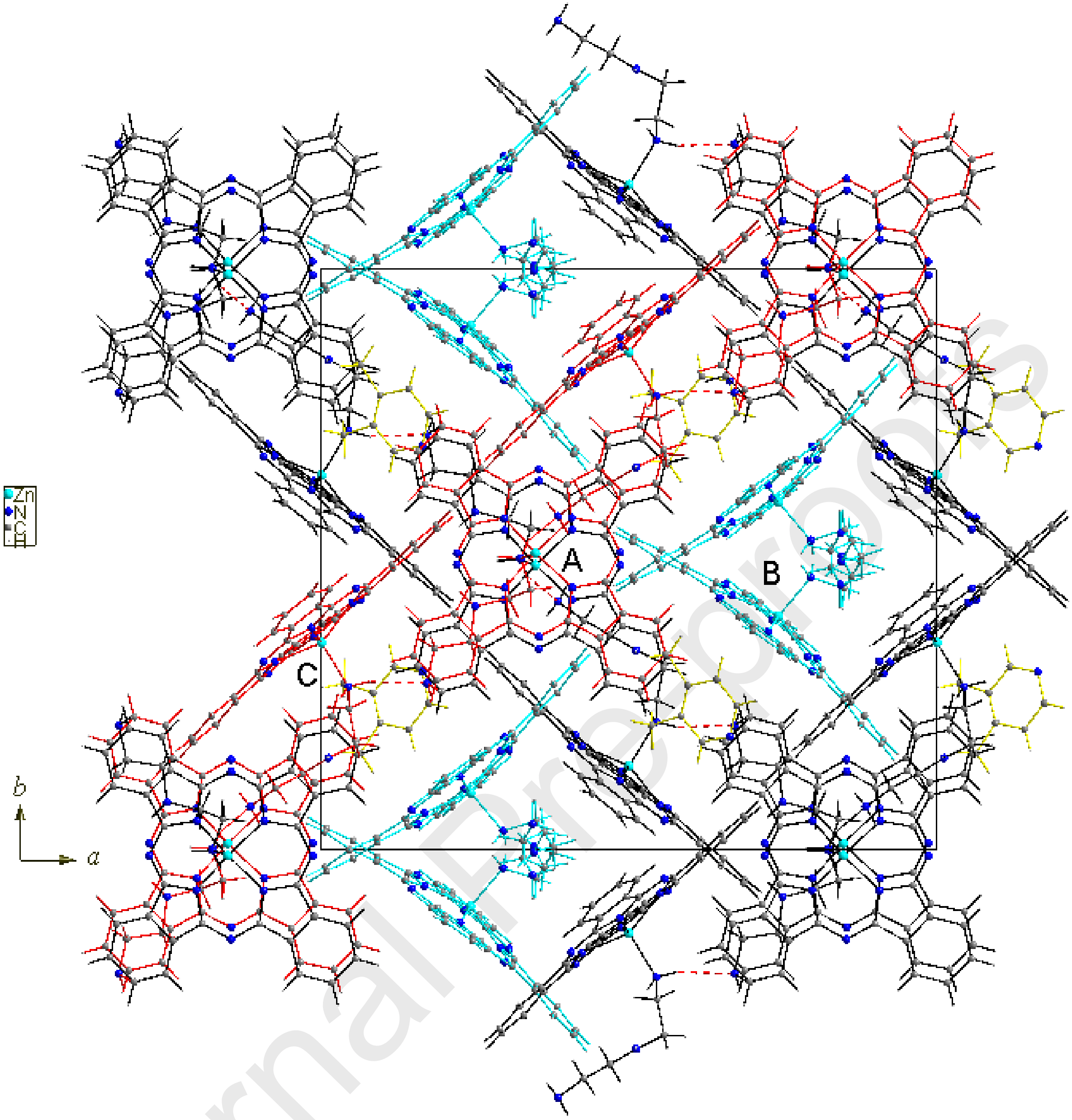

Figure 5. Packing diagram of **1** showing N-H···N hydrogen boned chains consisting of molecules A and C (one of them parallel to [110] direction is marked in red) and of molecules B (blue chains parallel to [001] direction), and the solvated 3,4-lutidine molecules are marked in yellow.

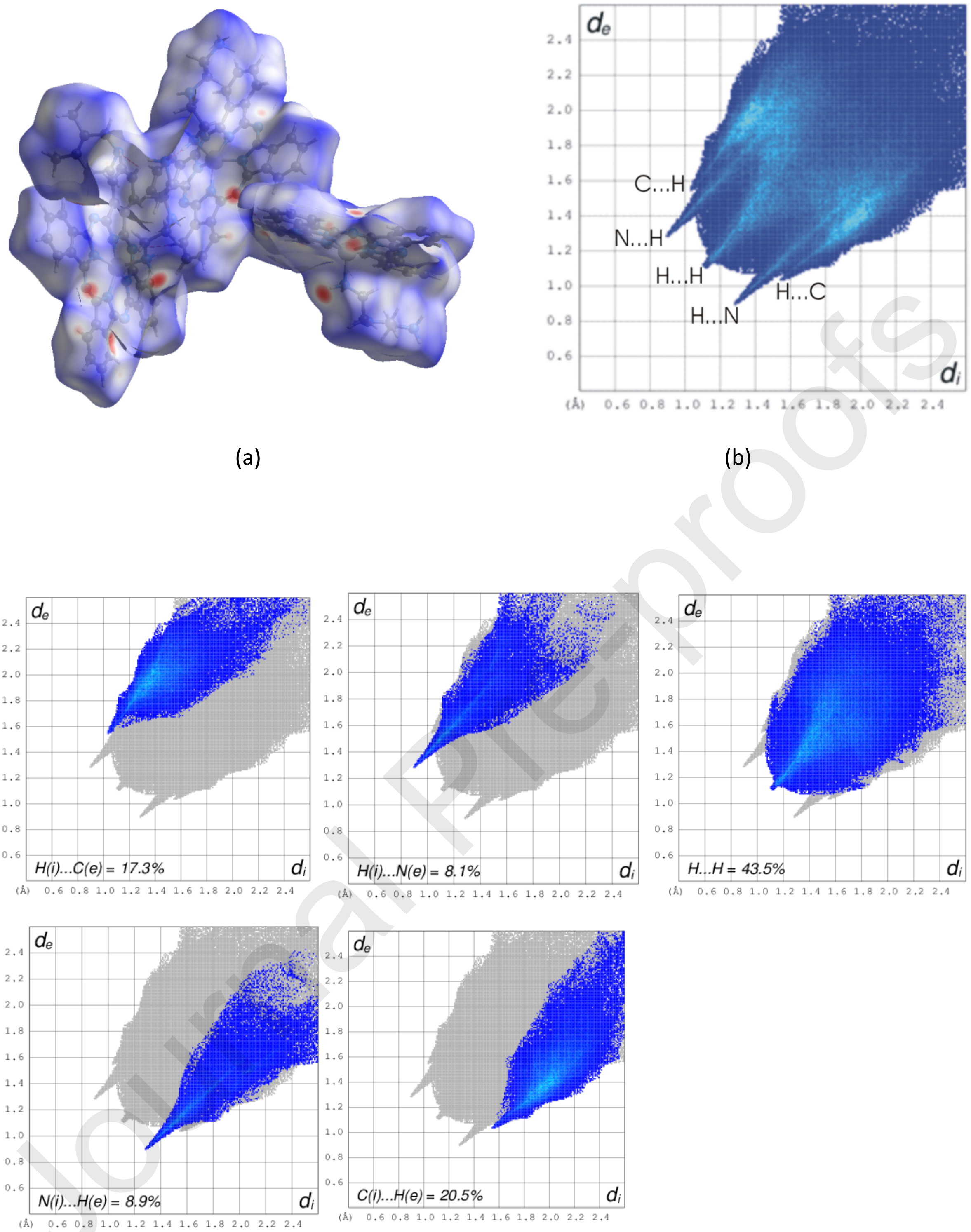

(a)

(b)

(c)

Figure 6. Hirshfeld surface (a) and the total fingerprint plot (b) for the asymmetric unit of **1**, and the fingerprint plot corresponding to respective interactions and their percentage contributions in the total interactions.

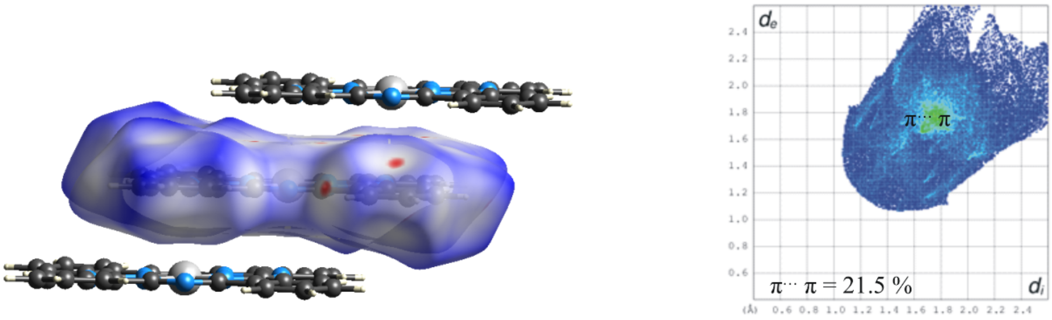

(a) (b)

Figure 7. Hirshfeld surface (a) and the total fingerprint plot (b) for the ZnPc in the crystal of β-form.

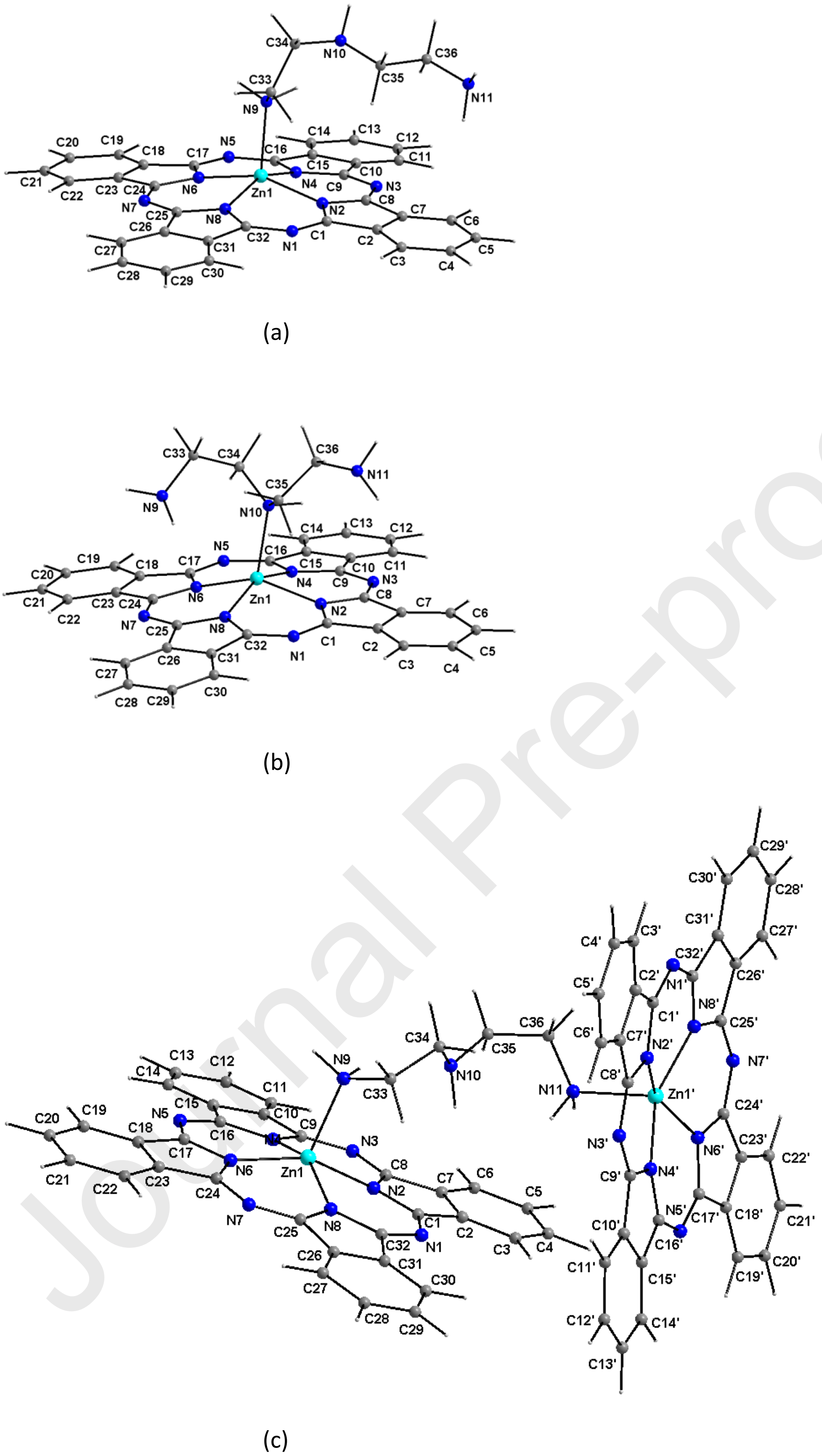

(a)

(b)

(c)

Figure 8. View of the DFT optimized structure of ZnPc coordinated by diethylenetriamine: (a) with terminal amine group, (b) with the central amine group and (c) bridged by terminal amine group.

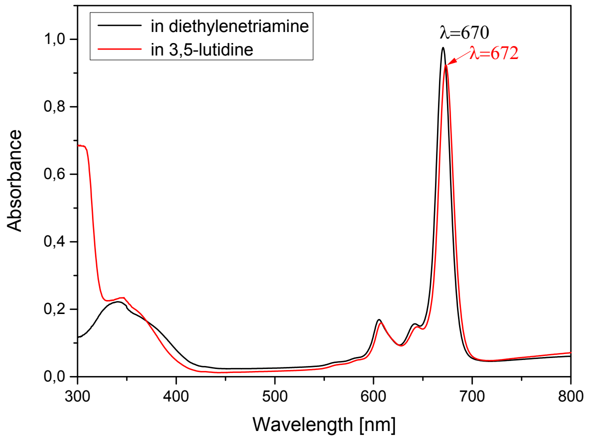

(a)

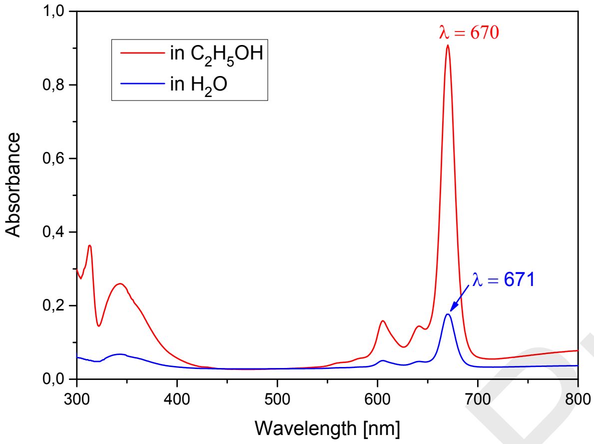

(b)

Figure 9. UV-Vis spectrum of (**1**) in diethylenetriamine and in 3,4-lutidine solutions (a) and in ethanol and in water solutions (b).

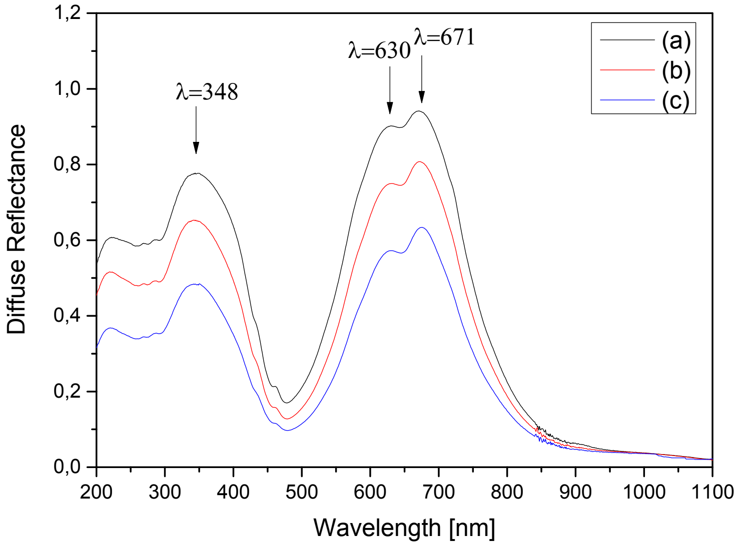

Figure 10. UV-Vis diffuse reflectance spectrum of (**1**) diluted with Al_2O_3 with a mass ratio of 1:20 (a), 1:40 (b) and 1:60 (c).

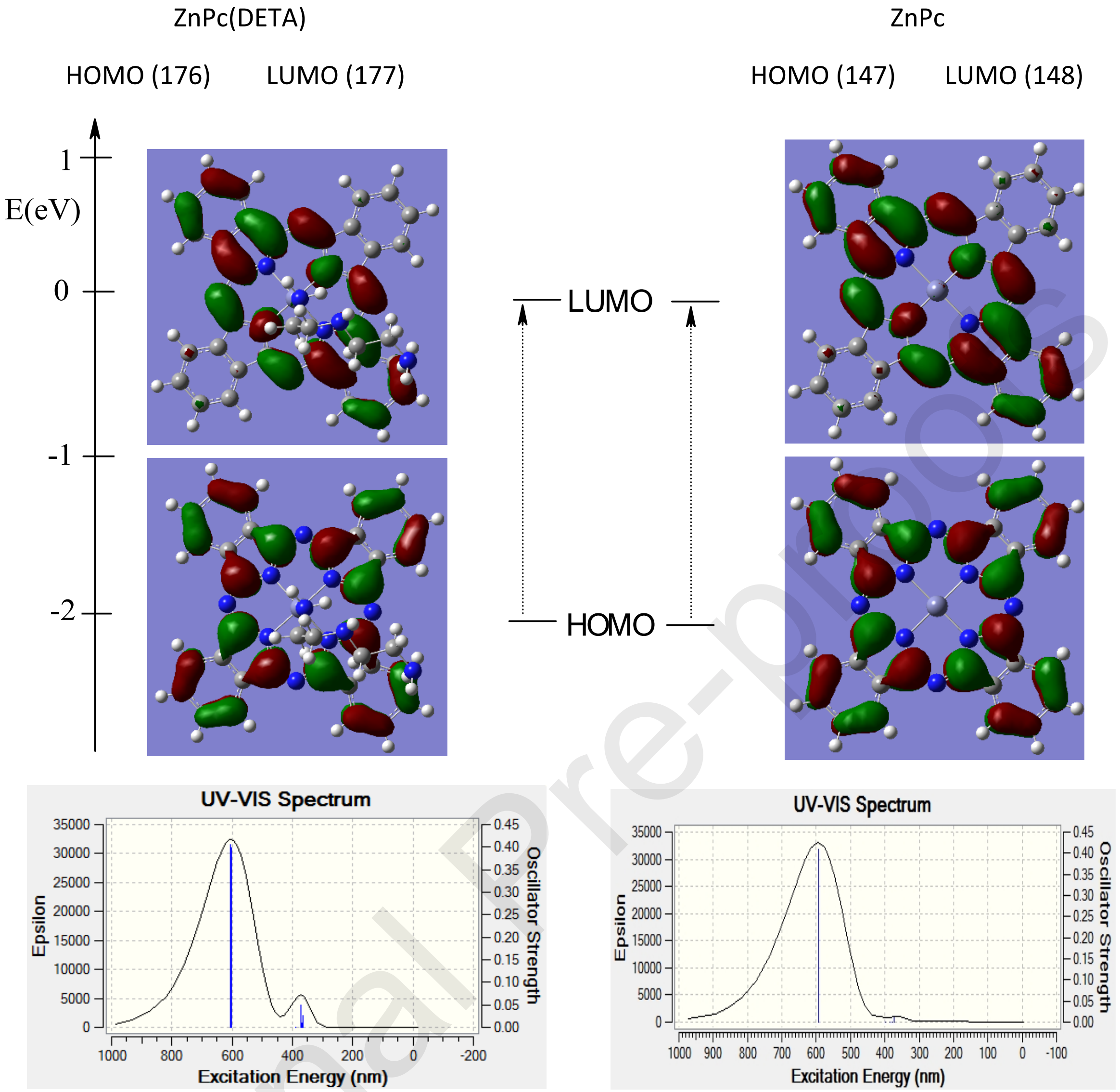

ΔE(HOMO/LUMO) = 2.0251 eV (612 nm)

ΔE(HOMO/LUMO) = 2.0857 eV (594 nm)

Figure 11. Partial molecular energy diagram, HOMO and LUMO frontiers orbitals and the calculated absorption spectra for the ZnPc(DETA) and ZnPc for a comparison.

References

[1] M.A. Dahlen, "The Phthalocyanines A New Class of Synthetic Pigments and Dyes". *Industrial Engineering Chemistry* **31** (1939) 839–847.

[2] M.J. Stillman, T. Nyokong: *Phthalocyanines, Properties and Applications*, ed. by C.C. Leznoff, A.B.P. Lever, VCD, New York 1989, Chapt. 3;

[3] (a) J.H. Sharp and L. Miller, *J. Phys. Chem*. **72** (1968) 3335-3337; (b) R. Kubiak, J.Janczak, K. Ejsmont, *Chem. Phys. Lett*. **245** (1995) 249-252; (c) F. Iwatsu, *J. Phys. Chem*. **92** (1988) 1678-1681.

[4] (a) F. Ghani, J. Kristen, H. Riegler, *J. Chem. Eng. Data*. **57** (2012) 439–449.

[5] F. Dumoulin, M. Durmuş, V. Ahsen, T. Nyokong, *Coord. Chem. Rev*. **254** (2010) 2792-2847.

[6] (a) F.H. Moser, A.L. Thomas, *The Phthalocyanines*, CRC, Boca Raton, FL, 1983; (b) N B. McKeown, *Phthalocyanine Materials*, Cambridge University Press, 1998; (c) M. Gouterman, P. Sayer, E. Shankland, J.P. Smith, *Inorg. Chem*. **20** (1981) 87-92; (d) M. Fujiki, H. Tabei, K. Isa, *J. Am. Chem. Soc*. **108** (1986) 1532-1536; (e) P. Sayer, M. Gouterman, C. R. Connell, *Acc. Chem. Res*. **15** (1982) 73-79; (f) J. Li, L.R. Subramanian, M. Hanack, Eur. J. Org. Chem. 1998,275922767

[7] (a) V.P. Singh, B. Parsarathy, R.S. Singh, A. Aguilera, J. Anthony, M. Payne, *Sol. Energy Mater. Sol. Cells* 90 (2006) 798-812; (b) W.P. Jakubik, *Thin Solid Films* **517** (2009) 6188–6191; (c) S. Pfuetzner, J. Meiss, A. Petrich, M. Riede, K. Leo, *Appl. Phys.Lett.* **94** (2009) 253303; (d) A. Medina, C.G Claessens, *J. Porphyrins Phthalocyanines* **13** (2009) 446–454; (e) S. Kato, H. Moriyama, K. Takahashi, C. Pac, *J. Mater. Chem.* **19** (2009) 8403–8410; (f) L. Rapp, A.K. Diallo, A.P. Alloncle, C. Videlot-Ackermann, F. Fages, P. Delaporte, *Appl. Phys. Lett.* **95** (2009) 171109; (g) Y. Ohmori, H. Kajii, *Proc. IEEE* **97** (2009) 1627–1636.

[8] (a) J.D. Myers, T.K. Tseng, J. Xue, *Org. Electron.* **10** (2009) 1182–1186; (b) R.B. Ye, M. Baba, K. Suzuki, K. Mori, *Thin Solid Films* **517** (2009) 3001–3004.

[9] (a) B. Tunhoo, J. Nukeaw, *Mater. Res. Innovations* **13** (2009) 145–148; (b) H. Benten, N. Kudo, H. Ohkita, S. Ito, *Thin Solid Films* **517** (2009) 2016–2022.

[10] (a) M.L Rodriguez-Mendez, J.A. de Saja, *J. Porphyrins Phthalocyanines* **13** (2009) 606–615; (b) W.S. Alencar, F.N. Crespilho, M.R.M.C. Santos, V. Zucolotto, N.R, Jr. Oliveira, W.C. Silva, *J. Phys. Chem. C* **111** (2007) 12817–12821.

[11] F. Bachmann, R.W. Basler, C. Dosenbach, M. Jeevanath, A. Kaeser, H. Kramer, N.J. Lant, G.S. Miracle, G. Roentgen, Patent No. WO2009069077-A2, 04 June 2009.

[12] T. Fujii, K. Hirota, Patent No. WO2009133668-A1, 05 Nov 2009.

[13] (a) P. Gregory, High-Technology Applications of Organic colorants: CRC Press: Boca Ratopn, Fl., 1983; (b) P. Gregory, *J. Porphyrins Phthalocyanines* **4** (2000) 432–437.

[14] (a) A.B. Sorokin, "Phthalocyanine Metal Complexes in Catalysis". *Chem. Rev*. **113** (2013) 8152–8191; (b) J. Janczak, *Polyhedron* **38** (2012) 75-87.

[15] (a) J.D. Spikes, *Photochem. Photobiol.* **46** (1986) 6910699. (b) I.J. MacDonald, T.J. Dougherty, *J. Porphrins Phthalocyanines* **5** (2001) 105–129; (c) H. Ali, J.E. van Lier, *Chem. Rev*. **99** (1999) 2379–2450; (d) R. Bonnett, *Chem. Soc. Rev*. **24** (1995) 19–33; (e) J.D. Miller, E.D. Baron, H. Scull, A. Hsia, J.C. Berlin, T. McCormick, V. Colussi, M.E. Kenney, K.D. Cooper, N.L. Oleinick, *Toxicol Appl Pharmacol.* **224** (2007) 290-299; (f) T. Nyokong, E. Antunes, Photochemical and photophysical properties of metallophthalocyanines, in: K.M. Kadish, K.M. Smith, R. Guilard (Eds.), The Handbook of Porphyrin Science, Vol. 7, World Scientific Press, Singapore, 2010, pp. 247.

[16] (a) M. Hanack, A. Gül, A. Hirsch, B.K. Mandal, L.R. Subramanian, W. Witke, *Mol. Crys. Liq. Cryst*. **187** (1990) 365-382; (b) M.P. Donzello, Z. Ou, D. Dini, M. Meneghetti, C. Ercolani, K.M. Kadish, *Inorg. Chem*. **43** (2004) 8637-8648; (c) X. Deng, W.W. Porter, T.P. Vaid, *Polyhedron*, 24 (2005) 3004-3011; (d) F. Yuksel, D. Atilla, V. Ahsen, *Polyhedron*, **26** (2007) 4551-4556; (e) J. Mack, N. Kobayashi, *Chem. Rev*. **111** (2011) 281-321; (f) E. Tuğba, D. Çakir, Z. Biyiklioğlu, H. Kantekin, *Dyes Pigments*, 98 (2013) 255-262; (g) H. Dumrul, F. Yuksel, *Polyhedron*, **63** (2013) 83-90.

[17] (a) J. Janczak, R, Kubiak, *Polyhedron*, **21** (2002) 265-274; (b) R. Kubiak, J. Janczak, M. Śledź, E. Bukowska, *Polyhedron*, **26** (2007) 4179-4186; (c) J. Janczak, R. Kubiak, E. Bukowska, *J. Mol. Struct.*, **937** (2009) 25-33; (d) J. Janczak, R. Kubiak, *J. Mol. Struct.* **935** (2009) 53-59; (e) J. Janczak, R. Kubiak, *CrystEngComm*, **12** (2010) 3599-3606; (f) J. Janczak, *Polyhedron* **30** (2011) 2933-2940; (g) J. Janczak, R. Kubiak, J. Lisowski, *Polyhedron* **30** (2011) 253-258; (h) J. Janczak, R. Kubiak, *J. Coord. Chem*. **65** (2012)

2478-2488; (i) J. Janczak, R. Kubiak, J. Lisowski, *J. Porphyrins Phthalocyanines*, **17** (2013) 742-749; (j) J. Janczak, R. Kubiak, *Eur. J. Inorg. Chem*. (2014) 1105-1115.

[18] (a) V.I. Vlaskin, O.P. Dimitriev, Z.I. Kazantseva, A.V. Nabok, *Thin Solid Films*, **286** (1996) 40-44; (b) H. Isago, C.C. Leznoff, M.F. Pyan, R.A. Metcalfe, R. Davids, A.B.P. Lever, *Bull. Chem. Soc. Jpn*. **71** (1998) 1039-1047; (c) K. Adachi, H. Watarai, *Bull. Chem. Soc. Jpn*. **77** (2004) 2011-2020.

[19] (a) B. Przybył, J. Janczak, *Dyes Pigments*, **100** (2014) 247-254; (b) J. Janczak, *Polyhedron* **70** (2014) 164-171; (c) B. Przybył, J. Janczak, *Dyes Pigments* **118** (2015) 102-109; (d) B. Przybył, J. Janczak, *Dyes Pigments*, **130** (2016) 54-62; (d) V. Kinzhybalo, R. Kubiak, J. Janczak, *Polyhedron* **115** (2016) 142-154.

[20] (a) Q. Zeng, D. Wu, C. Wang, J. Lu, B. Ma, C. Shu, H. Ma, Y. Li, C. Bai, *CrystEngComm*, 7 (2005) 243-248; (b) J. Janczak, R. Kubiak, *Polyhedron* **28** (2009) 2391-2396.

[21] R. Kubiak, J. Janczak, *J. Alloys Comp*. **200** (1993) L7-L8.

[22] CrysAlis CCD and CrysAlis Red 1.171.38.43, Rigaku Oxford Diffraction, 2015.

[23] (a) G.M. Sheldrick, *Acta Cryst*. A71 (2015) 3-8; (b) G.M. Sheldrick, *Acta Cryst.* C**71** (2015) 3-8.

[24] K. Brandenburg, H. Putz, DIAMOND Version 3.0, Crystal Impact GbR, Bonn, Germany, (2006).

[25] S.K. Wolff, D.J. Grimwood, J.J. MacKimon, M.J. Turner, D. Jayatilaka, A.M. Spackman, Crystal Explorer ver. 3.1, University of Western Australia, Perth, Australia, 2013.

[26] M. J. Frisch, G. W. Trucks, H. B. Schlegel, G. E. Scuseria, M. A. Robb, J. R. Cheeseman, G. Scalmani, V. Barone, B. Mennucci, G. A. Petersson, H. Nakatsuji, M. Caricato, X. Li, H. P. Hratchian, A. F. Izmaylov, J. Bloino, G. Zheng, J. L. Sonnenberg, M. Hada, M. Ehara, K. Toyota, R. Fukuda, J. Hasegawa, M. Ishida, T. Nakajima, Y. Honda, O. Kitao, H. Nakai, T. Vreven, J. A. Montgomery, Jr., J. E. Peralta, F. Ogliaro, M. Bearpark, J. J. Heyd, E. Brothers, K. N. Kudin, V. N. Staroverov, T. Keith, R. Kobayashi, J. Normand, K. Raghavachari, A. Rendell, J. C. Burant, S. S. Iyengar, J. Tomasi, M. Cossi, N. Rega, J. M. Millam, M. Klene, J. E. Knox, J. B. Cross, V. Bakken, C. Adamo, J. Jaramillo, R. Gomperts, R. E. Stratmann, O. Yazyev, A. J. Austin, R.

Cammi, C. Pomelli, J. W. Ochterski, R. L. Martin, K. Morokuma, V. G. Zakrzewski, G. A. Voth, P. Salvador, J. J. Dannenberg, S. Dapprich, A. D. Daniels, O. Farkas, J. B. Foresman, J. V. Ortiz, J. Cioslowski, and D. J. Fox, Gaussian, Inc., Wallingford CT, 2013. Gaussian16, Revision B.01, Gaussian, Inc., Wallingford, CT, 2016.

[27] (a) A. D. Becke, *J. Chem. Phys*. **104** (1996) 1040-1046; (b) C. Lee, W. Yang, R. G. Parr, *Phys. Rev*. B**37** (1988) 785-789; (c) B. G. Parr, W. Yang, Density-functional Theory of Atoms and Molecules, Oxford University Press, New York, 1989.

[28] (a) R. Ditchfield, W.J. Hehre, J.A. Pople, *J. Chem. Phys*. **54** (1971) 724-728; (b) W.J. Hehre, R. Ditchfield, J.A. Pople, *J. Chem. Phys*. **56** (1972) 2257-2261; (c) P.C. Hariharan, J.A. Pople, *Theor. Chim. Acta* **28** (1973) 213-222; (d) P.C. Hariharan, J.A. Pople, *Mol. Phys*. **27** (1974) 209-214; (e) M.S. Gordon, *Chem. Phys. Lett*. **76** (1980) 163-168.

[29] (a) R. Bauernschmitt, R. Ahlrichs, *Chem. Phys. Lett*. **256** (1996) 454-464; (b) A. Dreuw, M. Head-Gordon, *Chem. Rev*. **105** (2005) 4009-4037.

[30] (a) S.K. Kurtz, T.T. Perry, *J. Appl. Phys.* 1968, 39 (8), 3798-3813; (b) A. Graja, *Phys. Status Solidi* (b) 1968, 27 (2), K93-K97.

[31] (a) J.K. Zaręba, M.J. Białek, J. Janczak, M. Nyk, J. Zoń, M. Samoć, *Inorg. Chem.*, 54 (2015) 10568-10575. (b) J.K. Zaręba, J. Janczak, M. Samoć, M. Nyk, *Dalton Trans.*, 46 (2017) 9349-9357.

[32] (a) P. Politzer, P.R. Laurence, K. Jayasuriya, *Environ. Health Perespect*. **61** (1985) 191-202; (b) P. Politzer, P. Lane, *Struct. Chem*. **1** (1990) 159-164.

[33] (a) P. Sjoberg, P. Politzer, *J. Phys. Chem*. **94** (1990) 3959-3961; (b) P. Politzer, J. S. Murray, In *Comput. Med. Chem. Drug Discovery.* P. Bultinck, P. H. De Winter, W. Langenaeker, J. P. Tollenaere, (Eds.) New York: Marcel Dekker Inc; 2004. pp. 213–234; (c) C. A. Hunter, *Angew. Chem., Int. Ed*. **43** (2004) 5310-5324.

[34] W.R. Scheidt, W. Dow, *J. Am. Chem. Soc*. **99** (1977) 1101-1104.

[35] F.H. Allen, *Acta Cryst*. B**58** (2002) 380–388.

[36] A.M. Spackman, D. Jayatilaka, *CrystEngComm*, **11** (2009) 19-32.

[37] J.J. MacKimon, A.M. Spackman, A.S. Mitchell, *Acta Cryst*. B**60** (2004) 627-668.

[38] J.J. MacKimon, D. Jayatilaka, A.M. Spackman, *Chem. Commun*. **37** (2007) 3814-3816.

[39] M.-S. Liao, S. Scheiner, *J. Chem. Phys.* **114** (2001) 9780-9781.

[40] (a) L. Edwards, M. Gouterman, *J. Mol. Spectrosc*. **1970**, *33*, 292-310; (b) K.M. Kadish, D.J. Leggett, D. Chang, *Inorg. Chem.* **1982**, *21*, 3618-3622.

[41] (a) T. Nykong, Z. Gasyna, M.J. Stillman, *Inorg. Chem*. **1987**, *22*, 1087-1095; (b) T. Reinot, J.M. Hayes, G.J. Smal, C. Zerner, *Chem. Phys. Lett.* **1999**, *299*, 410-416; (c) K. Liu, Y. Wang, J. Yao, Y. Luo, *Chem. Phys. Lett*. **2007**, *438*, 36-40.

[42] (a) A. Endo, S. Matsumoto, J. Mizuguchi, *J. Phys. Chem.* A **103** (1999) 8193-8199; (b) J. Janczak, Y. M. Idemori, *Polyhedron* **22** (2003) 1167-1181; (c) J. Spadavecchia, G. Ciccarella, R. Rella, S. Capone, P. Siciliano, *Sensors and Actuators B: Chemical* **96** (2003) 489–49; (d) R.J.C. Brown, A.R. Kucernak, N.J. Long, C. Mongay-Batalla, *New J. Chem*. **28** (2004) 676-680; (e) Y. Açıkbaş, M. Evyapan, T. Ceyhan, R. Çapan, Ö. Bekaroğlu, *Sensors and Actuators B: Chemical* **123** (2007) 1017-1024; (f) B.W. Caplins, T.K. Mullenbach, R.J. Holmes, D.A. Blank, *Phys.Chem.Chem.Phys*. 18 (2016) 11454-11459; (g) K.J. Hamam1, M.I. Alomari, *Appl. Nanosci*. **7** (2017) 261-268.

[43] (a) Y. Yang, *J. Phys. Chem*. B **112** (2011) 9043-9054; (b) J. Janczak, *Inorg. Chim. Acta* **478** (2018) 88-103; (c)) J. Janczak, *ACS Omega* **4** (2019) 3673-3683.

[44] (a) J. Mack, M.J. Stillman, *J. Am. Chem. Soc.* **116** (1994) 1294-1304; (b) J. Mack, M.J. Stillman, *Inorg. Chem.* **36** (1997) 413–425; (c) G. Ricciardi, A. Rosa, E.J. Baerends, *J. Phys. Chem. A,* **105** (2001) 5242–5254; (d) J. Mack, Y. Asano, N. Kobayashi, M.J. Stillman, *J. Am. Chem. Soc*. **127** (2005) 17697-17711; (e) M. Pia Donzello, C. Eroclani, K.M. Kadish, G. Ricciardi, A. Rosa, P.A. Stuzhin, *Inorg. Chem*. **46** (2007) 4145-5157; (f) X. Liang, J. Mack, L.M. Zheng, Z. Shen, N. Kobayashi, *Inorg. Chem.* **53** (2014) 2797–2802; (g) J. Mack, *Chem. Rev.* **117** (2017) 3444–3478; (h) I. Lanzao, N. Russo, E. Sicilia, *J. Phys. Chem.* B, **112** (2008) 4123-4130; (i) J. Mack, J. Stone, T. Nyokonmg, *J. Porphrins Phthalocyanines* **18** (2014) 630-641.

[45] (a) G. Ricciardi, A. Rosa, E.J. Baerends, *J. Phys. Chem.* A **105** (2001) 5242-5254; (b) A. Rosa, G. Ricciardi, *Can. J. Chem*. **87** (2009) 994-1005; (c) L.T. Ueno, C.C. Jayme, L. R. Silva, E. B. Pereira, S.M. Oliveira, A.E.H. Machado*, J. Braz. Chem. Soc*. **23** (2012) 2237-2247; (d) R.F. Theisen, L. Huang, T. Fleetham, J.B. Adams, J. Li, *J. Chem. Phys*. **142** (2015) 094310, doi: 10.1063/1.4913757.

[46] (a) W. Liu, T.J. Jensen, F.R. Fronczek, R.P. Hammer, K.M. Smith, A.G.H. Vicente, *J. Med. Chem*. **48** (2005) 1033-1041; (b) S. Makhseed, M. Machacek, W. Alfadly, A. Tuhl, M.

Vinodh, T. Simunek, V. Novakova, P. Kubat, E. Rudolf, P. Zimcik, Chem.Commun., 49 (2013) 11149-11151; (c) S. Moeno, R.W. Krause, E.A. Ermilov, W. Kuzyniak, M. Höpfner, Photochem. Photobiol. Sci. 13 (2014) 963-970; (d) T. Ikeuchi, J. Mack, T. Nyokong, N. Kobayashi, M. Kimura, *Langmuir*, **32** (2016) 11980-11985.

[47] (a) K.M. Ok, E.O. Chi, P.S. Halasyamani, *Chem. Soc. Rev.* **35** (2006) 710−717; (b) D.D. Huang, R.G. Xiong, *Polyhedron* **16** (1997) 3929−3939; (c) R.G. Xiong, X. Xue, H. Zhao, X.Z. You, B.F. Abrahams, Z.L. Xue, *Angew. Chem., Int. Ed.* **41** (2002) 3800−3803.

[48] (a) G. De la Torre, P. Vázquez, F. Agulló-López, T. Torres, *Chem. Rev*. **104**, (2004) 3723-3750; (b) S.R. Flom, In Porphyrin Handbook; K.M. Kadish, K.M. Smith, R. Guilard, (Eds.); Academic Press: Boston, MA, 2003; Vol. 19, p 179.

Author Contributions Section

I am the only author

Declaration of interests

☒ The authors declare that they have no known competing financial interests or personal relationships that could have appeared to influence the work reported in this paper.

☐The authors declare the following financial interests/personal relationships which may be considered as potential competing interests:

Highlights

- Coordination properties of diethylenetriamine in relation to ZnPc have been investigated.
- ZnPcDETA complex was obtained in the crystalline form as 3,4-lutidine solvate.
- Ligation *via* terminal is energetically more favorable than through the central amino group of DETA.
- HS and the 2D-fingerprint plots were analysed in comparison to that of parent ZnPc.
- MO energy diagrams and the calculated absorption spectra of ZnPcDETA are reported.
- Solubility of the ZnPcDETA is significantly greater than the parent ZnPc pigment.
- ZnPcDETA that crystallizes in non-centrosymetric space group exhibits SHG.

Graphical Abstract Picture

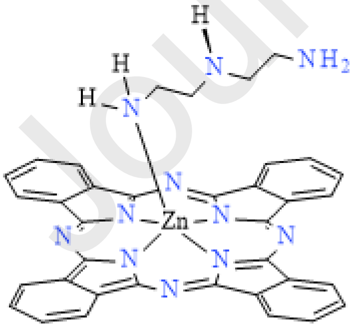

Graphical Abstract Text

The coordination properties of diethylenetriamine (DETA) as a ligand containing three donor nitrogen atoms, two terminal primary amino groups and one secondary central amino group, with respect to divalent zinc ion in ZnPc were examined. ZnPcDETA complex (**1**) in which the DETA coordinates via terminal amine group was characterized by X-ray single crystal analysis. The lack of π ... π interactions between phthalocyanine(2-) macrocycles in crystals **1** significantly increases their solubility in most common solvents, and even in water, compared to the parent ZnPc pigment with limited solubility in solvents and insoluble in water.